

100  
101  
102  
103  
104  
105  
106  
107  
108  
109  
110  
111  
112  
113

# One-Class Multiple-Look Fusion: A theoretical comparison of different approaches with examples from infrared video

150  
151  
152  
153  
154  
155  
156  
157  
158  
159156  
157  
158  
159  
160  
161  
162  
163  
164  
165  
166  
167  
168  
169  
170  
171  
172  
173  
174  
175  
176  
177  
178  
179  
180  
181  
182  
183  
184  
185  
186  
187  
188  
189  
190  
191  
192  
193  
194  
195  
196  
197  
198  
199

## Abstract

Multiple-look fusion is quickly becoming more important in statistical pattern recognition. With increased computing power and memory one can make many measurements on an object of interest using, for example, video imagery or radar. By obtaining more views of an object, a system can make decisions with lower missed detection and false alarm errors. There are many approaches for combining information from multiple looks and we mathematically compare and contrast the sequential probability ratio test, Bayesian fusion, and Dempster-Shafer theory of evidence. Using a consistent probabilistic framework we show how to transform results from one approach to the other and show results for an application in infrared video classification.

128  
129  
130

## 1. Introduction

There have long been multiple competing approaches for accomplishing multiple look sensor fusion. By multiple look fusion we assume we can make multiple measurements on an object, as it passes through the field of view of the sensor. For example, multiple frames in an infrared video or the extraction of multiple high-resolution-range profiles from ground-moving-target-indicator radar.

131  
132  
133  
134  
135  
136  
137  
138  
139  
140  
141  
142  
143  
144  
145  
146  
147  
148  
149

Here, we will theoretically compare and contrast three data fusion approaches: sequential probability ratio test (SPRT), Bayesian, and Dempster Shafer (DS). To accomplish this we will use a common probabilistic framework that is useful in real-world pattern recognition problems in unconstrained environments. Our goal is not to say one is better than the other, but to find commonalities between the various approaches and use one approach to find insights into others. This can eventually lead to a unified approach in sensor fusion.

## 2. One Class Classifiers

A structure one might choose for a classification

problem is based on a *one-class* classifier [1]. For one class classifiers, we are interested in one specific target  $\theta_1$  represented by the alternative hypothesis  $H_1$ , and the null hypothesis  $H_0$  represents the non-target  $\bar{\theta}_1$  class. While this might seem like an over simplification, one could argue that for a multi-class problem with other targets of interest  $\theta_2, \dots, \theta_m$  one would design a one-class classifier for each of them. For the  $\theta_1$  one-class classifier we can further divide the nontargets into two groups: the other targets of interest  $\theta_2, \dots, \theta_m$  and the unknown class  $\theta_0$ . This allows us to further distinguish between two types of false alarm errors: *between-class* and *out-of-class*. Between-class errors occur when alarming on another target  $\theta_2, \dots, \theta_m$  by calling it the target  $\theta_1$ . Out-of-class errors occur when alarming on an unknown signature  $\theta_0$  by calling it the target  $\theta_1$ . In making any decision, we want to control two types of errors: *missed detection errors* and *false alarm errors*. Missed detection errors result from missing a target signature by calling it a nontarget, and false alarm errors result from alarming on a nontarget signature by calling it a target.

For example, suppose we are interested in classifying moving objects in infrared video as humans, vehicles, or unknown. Here,  $\theta_1$  would represent the human class and  $\theta_2$  the vehicle class. The unknown class  $\theta_0$  would represent all moving objects not in  $\theta_1$  or  $\theta_2$ . This would be wind-blown objects (tumble weed, boxes, trash cans, etc.) or animals. These unknown moving objects, a possible source of the out-of-class errors, are a significant problem in real-world pattern recognition problems in unconstrained environments. A Bayesian classifier approach designed for the human vs. vehicle problem, while minimizing the between-class errors, would require models of all the possible objects that could be imaged by the sensor to control the out-of-class errors. Otherwise it would classify an animal as human or vehicle. Modeling “the whole world” of possible objects is untenable for most realistic systems deployed in unconstrained environments. Instead, we use a goodness of fit (GOF)

200 classifier to control the out-of-class errors, and power  
 201 analysis [8] to model the unknown class.

Whereas Bayesian classifiers minimize the between-class error, they do nothing to control the out-of-class errors. Figure 1 illustrates this potential problem. The figure shows a two-dimensional feature space, with samples from two targets: Target *A* represented by stars and Target *B* represented by filled circles. Assuming normal distributions and equal covariance matrices for the targets, the Bayes decision boundary has a linear form (Figure 1a). Whereas the Bayes classifier minimizes the between-class errors of the *A* and the *B* targets, it does not control the out-of-class errors caused by unknown objects represented by “*x*” symbols. Depending on which side of the boundary the nontarget falls, the classifier will assign the unknown to one of the known classes and make an out-of-class error. Figure 1b shows a GOF classifier that tries to surround the target class. Here, the unknown objects, that have widely differing features from the target class (“*x*” symbols), will be classified correctly. In general, the GOF classifier has improved out-of-class errors, but the between-class errors will increase, since it is not necessarily an optimal Bayes classifier.

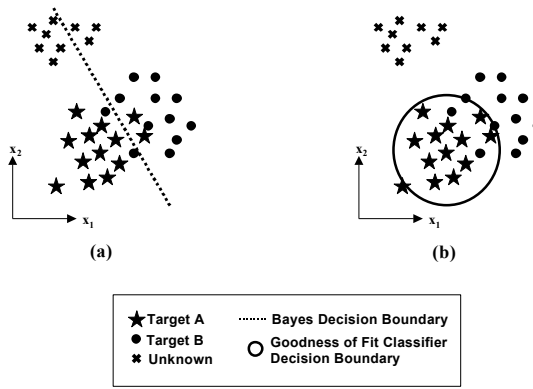


Figure 1: Comparison of Bayes and goodness of fit (GOF) classifiers. (a) Bayes classifier. (b) GOF classifier.

### 3. Probabilistic Framework

We will use the same probabilistic framework for comparing and contrasting the fusion algorithms. We start by assuming a stream of observations represented as random variables  $x_1, x_2, \dots$ . These samples result from the best match scores in the GOF metric. We also assume knowledge of the functions  $p(x_i | T)$  and  $p(x_i | \bar{T})$  which represent the probability density function (PDF) of an observation  $x_i$ , given the target  $T$  and the nontarget  $\bar{T}$ , respectively. The PDF's can be discrete or continuous and

be determined through theoretical means or empirical modeling. 29  
29

The PDF  $p(x_i | T)$  is usually straight forward to determine, since one has knowledge of the target of interest. This information can come from data collections or modeling and simulation using CAD descriptions and a physics-based sensor signature prediction software such as Irma [9]. The PDF  $p(x_i | \bar{T})$  is usually more problematic. One approach for modeling the nontarget class uses *statistical power analysis* [8] to model the *worst case nontarget*. The approach has some similarities to that taken by [1] for modeling composite hypotheses by determining the *least favorable choice*. Power analysis assumes the tested effect is linear and the measured effect size (small, medium or large) is known. Typically, power analysis allows the statistician to determine if enough samples were collected to give the test a high power. While the exact form depends on  $p(x_i | T)$ , we show an example from [5] where  $p(x_i | T)$  is  $N(0,1)$ . This is convenient in problems where the central limit theorem can be applied. In [5], it was shown that the worst case nontarget PDF is  $N(\mu_N, 1)$ . Here the location parameter  $\mu_N$  represents the smallest acceptable effective difference between the target and nontarget.

## 4. Sequential Probability Ratio Test

One approach for combining decisions as they become available is to use the Wald sequential hypothesis test or SPRT [11]. After  $n$  observations the likelihood ratio is:

$$\Lambda(n) = \prod_{i=1}^n \lambda_i, \quad \lambda_i = \frac{f(x_i | T)}{f(x_i | \bar{T})} \quad (1)$$

Often it is more numerically convenient to work with the log-likelihood:

$$Z(n) = \log(\Lambda(n)) = \sum_{i=1}^n z_i, \quad z_i = \log\left(\frac{p(x_i | T)}{p(x_i | \bar{T})}\right) \quad (2)$$

The SPRT uses two decision boundaries ( $a, b$ ) to make a decision:

$$\begin{array}{ll}
 \text{Reject } H_0 & \text{If } Z(n) \geq a \\
 \text{Accept } H_0 & \text{If } Z(n) \leq b \\
 \text{Get more data} & \text{If } b \leq Z(n) \leq a
 \end{array} \quad . \quad (3)$$

One desirable property of the SPRT is that the decision boundaries can be determined from the chosen error rates. Thus, these decision boundaries can be obtained using the desired false alarm rate,  $\alpha$ , and the missed detection rate,  $\beta$ :

$$a = \log \frac{1-\beta}{\alpha} \text{ and } b = \log \frac{\beta}{1-\alpha}. \quad (4)$$

300 It has been shown that the SPRT, on average, uses the  
 301 smallest number of observations to make a decision [11].  
 302 It is interesting to note that the a-priori probabilities  $p(T)$   
 303 and  $p(\bar{T})$  do not appear in the log-likelihood ratio (2).

## 305 5. Bayesian Fusion

306 A sequential update formula can be derived from Bayes  
 307 formula:

$$309 \quad p(T|x_1) = \frac{p(T)p(x_1|T)}{p(T)p(x_1|T) + (1-p(T))p(x_1|\bar{T})} \quad (5)$$

310 The quantity  $p(T|x_1)$  is the likelihood of target after one  
 311 observation  $x_1$ . By substituting  $p(T|x_1)$  for the prior  $p(T)$   
 312 and a new observation  $x_2$  for  $x_1$  in (5) we get the likelihood  
 313 of a target after two observations as:

$$318 \quad \frac{p(T)p(x_1|T)p(x_2|T)}{p(T)p(x_1|T)p(x_2|T) + (1-p(T))p(x_1|\bar{T})p(x_2|\bar{T})} \quad (6)$$

321 Using  $B(n)$  to represent the Bayesian likelihood after  $n$   
 322 observations or  $p(T|x_1 \dots x_n)$  we get

$$324 \quad Y(n) = \frac{\lambda_0 \Lambda(n)}{\lambda_0 \Lambda(n) + 1} \quad (7)$$

326 where  $\Lambda(n)$  is the Wald likelihood ratio in (1) and  $\lambda_0$   
 327 represents the a-priori likelihood ratio:

$$329 \quad \lambda_0 = \frac{p(T)}{(1-p(T))}. \quad (8)$$

331 The Bayesian likelihood is always between 0 and 1. By (1)  
 332 and the definition of a PDF  $0 \leq \Lambda(n) < \infty$ , so as  
 333  $\Lambda(n) \rightarrow \infty$  then  $Y(n) \rightarrow 1$  and if  $\Lambda(n) = 0$  then  $Y(n) = 0$ .  
 334 Also if the PDF's are discrete then we can compute a  
 335 Bayesian probability of a target. We can use the SPRT  
 336 stopping conditions to determine thresholds on the  
 337 Bayesian likelihood. If

$$339 \quad a = \log(A) \text{ and } b = \log(B) \quad (9)$$

340 then  $A$  and  $B$  are the upper and lower stopping  
 341 conditions for  $\Lambda(n)$ , respectively. Thus the Bayesian  
 342 stopping rule becomes:

$$343 \quad \begin{aligned} \text{Reject } H_0 & \quad \text{If } Y(n) \geq C \\ 344 \quad \text{Accept } H_0 & \quad \text{If } Y(n) \leq D \\ 345 \quad \text{Get more data} & \quad \text{If } C \leq Y(n) \leq D \end{aligned} \quad (10)$$

346 where

$$348 \quad C = \frac{\lambda_0}{1+\lambda_0} A = \frac{\lambda_0}{1+\lambda_0} \frac{(1-\beta)}{\alpha} \quad (11)$$

349 and

$$350 \quad D = \frac{\lambda_0}{1+\lambda_0} B = \frac{\lambda_0}{1+\lambda_0} \frac{\beta}{1-\alpha}. \quad (12)$$

351 Note the  $\lambda_0/(1+\lambda_0)$  basically tweaks the threshold  
 352 according to the a-priori information. For  $\lambda_0 > 1$  the  
 353 thresholds will go lower to make target calls slightly more  
 354 probable and if  $\lambda_0 < 1$  the thresholds will go higher to  
 355 make nontarget calls slightly more probable.

## 357 6. Dempster-Shafer Theory of Evidence

359 The Dempster Shafer (DS) theory [10] is a  
 360 mathematical theory of evidence that allows combining  
 361 evidence from different sources to arrive at a degree of  
 362 belief. It models uncertainty by not requiring one to assign  
 363 all of one's belief to a proposition.

366 The main assumption we make is that evidence is  
 367 *consonant*. This allows us to use the probabilistic  
 368 framework that we established in section 3. Shafer defines  
 369 consonant evidence as evidence that points in a single  
 370 direction and only varies in the precision of focus [10].  
 371 This fits well with the GOF metric. The GOF describes the  
 372 difference between stored knowledge, for example a  
 373 template of the target, and the measured data. Thus it  
 374 points only in the direction and focus of the hypothesis  
 375 represented by the stored knowledge.

376 For the one-class problem the frame of discernment is  
 377  $\Theta = \{T, \bar{T}\}$ . From [10] the support function for the target  
 378  $T$  is

$$381 \quad \left. \begin{aligned} m_x(\bar{T}) &= 0 \\ m_x(T) &= 1 - \frac{p(x|\bar{T})}{p(x|T)} \\ m_x(\Theta) &= \frac{p(x|\bar{T})}{p(x|T)} \end{aligned} \right\} \text{if } \frac{p(x|T)}{p(x|\bar{T})} > 1 \quad (13)$$

387 and the support for the nontarget  $\bar{T}$  is

$$388 \quad \left. \begin{aligned} m_x(\bar{T}) &= 1 - \frac{p(x|T)}{p(x|\bar{T})} \\ m_x(T) &= 0 \\ m_x(\Theta) &= \frac{p(x|T)}{p(x|\bar{T})} \end{aligned} \right\} \text{if } \frac{p(x|\bar{T})}{p(x|T)} > 1. \quad (14)$$

394 where  $m(\cdot)$  represents the DS basic probability assignment  
 395 (BPA) function and  $m_x(\Theta)$  represents the amount of  
 396 uncertainty in the observation  $x$ .

397 For what we want to show it is simpler to work with  
 398 DS's weight of evidence. If  $m(A)$  represents the BPA for  
 399 the proposition  $A \subseteq \Theta$  then weight of evidence  $w(A)$  is:

$$398 \quad w(A) = -\log(1-m(A)). \quad (15)$$

400 In terms of weight of evidence equation (13) becomes:  
 401  
 402  
 403  
 404  
 405

$$w_x(\bar{T}) = 0 \\ w_x(T) = \log\left(\frac{f(x|T)}{f(x|\bar{T})}\right) \text{ if } \frac{f(x|T)}{f(x|\bar{T})} > 1 \quad (16)$$

406 and equation (14) becomes  
 407  
 408  
 409

$$w_x(\bar{T}) = \log\left(\frac{f(x|\bar{T})}{f(x|T)}\right) \text{ if } \frac{f(x|\bar{T})}{f(x|T)} > 1 \\ w_x(T) = 0 \quad (17)$$

410 Using equation (2)  
 411  
 412

$$w_x(\bar{T}) = 0 \text{ if } \frac{f(x|T)}{f(x|\bar{T})} > 1 \\ w_x(T) = z \quad (18)$$

413 and  
 414

$$w_x(\bar{T}) = -z \text{ if } \frac{f(x|\bar{T})}{f(x|T)} > 1 \\ w_x(T) = 0 \quad (19)$$

415 where  $z$  represents the log-likelihood ratio in the SPRT. As  
 416 long as we separate the evidence and combine only  
 417 evidence supporting the same proposition, then we have  
 418 the homogenous weight of evidence combination rule  
 419 where the weights of evidence combine additively. For the  
 420 total support of the target class  $T$ , let  $w^+$  represent the  
 421 total amount of positive weight of evidence. Similarly  
 422 define  $w^-$  for the total support for the non-target class  $\bar{T}$ .  
 423 Here  
 424

$$w^+ = \sum_{i=1}^n w_{x_i}(T) = \sum_{i=1}^n z_i, \text{ for } \frac{f(x|T)}{f(x|\bar{T})} > 1 \text{ or } z_i > 0 \quad (20)$$

425 and  
 426

$$w^- = \sum_{i=1}^n w_{x_i}(\bar{T}) = \sum_{i=1}^n z_i, \text{ for } \frac{f(x|\bar{T})}{f(x|T)} > 1 \text{ or } z_i < 0 \quad (21)$$

427 Combining conflicting weights ( $w^+$  and  $w^-$ ) of evidence  
 428 cannot be done by simple addition. From [10] the weight  
 429 of evidence for the contradictory propositions  $T$  and  $\bar{T}$   
 430 becomes:  
 431

$$w(T) = \log\left(\frac{e^{w^+} + e^{w^-} - 1}{e^{w^-}}\right) \quad (22)$$

432 and  
 433

$$w(\bar{T}) = \log\left(\frac{e^{w^+} + e^{w^-} - 1}{e^{w^+}}\right). \quad (23)$$

434 Using (15) in reverse we can get the corresponding BPA  
 435 for propositions  $T$  and  $\bar{T}$   
 436

$$m(T) = \frac{e^{w^+} - 1}{e^{w^+} + e^{w^-} - 1} \quad (24)$$

437 and  
 438

$$m(\bar{T}) = \frac{e^{w^-} - 1}{e^{w^+} + e^{w^-} - 1} \quad (25)$$

439 The DS uncertainty is the BPA assigned to  $\Theta$  or  
 440

$$m(\Theta) = \frac{1}{e^{w^+} + e^{w^-} - 1} \quad (26)$$

441 Since  $m(T) + m(\bar{T}) + m(\Theta) = 1$  for a one-class classifier. Note  
 442 the uncertainty of the system's belief is driven down to 0  
 443 as evidence is collected or as  $w^+$  and/or  $w^-$  increase. Thus  
 444 high but equal  $w^+$  and  $w^-$  would give low uncertainty, but  
 445 an uninformed decision.  
 446

447 The most obvious decision rule is  
 448

$$\begin{aligned} \text{Decide } T & \text{ If } w(T) - w(\bar{T}) \geq 0 \\ \text{Decide } \bar{T} & \text{ otherwise} \end{aligned} \quad (27)$$

449 For the one-class problem, this turns out to be equivalent  
 450 to the three unambiguous decision rules proposed by Kim  
 451 in [4]. After some algebraic manipulation one can show  
 452 that (27) is equivalent to  
 453

$$\begin{aligned} \text{Decide } T & \text{ If } w^+ - w^- \geq 0 \\ \text{Decide } \bar{T} & \text{ otherwise} \end{aligned} \quad (28)$$

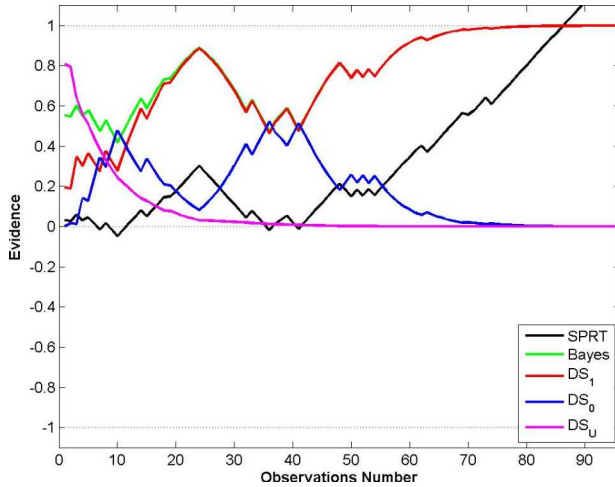
454 This is equivalent to a forced SPRT decision if one is  
 455 unwilling or unable to wait for any more observations.  
 456

## 7. Results

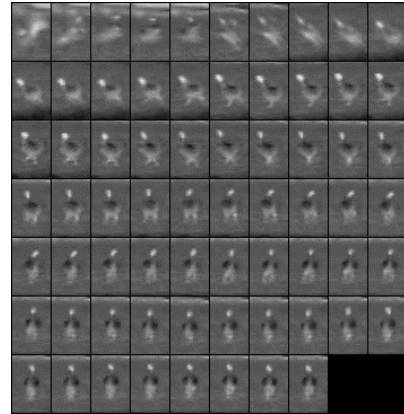
457 We show results on a one-class problem for video  
 458 motion classification (VMC). The target class  $T$   
 459 represents upright-human dismounts and the nontarget  
 460 class  $\bar{T}$  is any other mover detected by the video motion  
 461 detection (VMD) algorithm. The imager is an uncooled  
 462 DRS E3500 infrared camera with 320x240 resolution and  
 463 8-bit precision. VMD was accomplished with background  
 464 subtraction [1] and tracking with an alpha-beta tracker.  
 465 The features for VMC were histograms of oriented  
 466 gradients (HOG) [2] and the GOF metric was based on a  
 467 multinomial pattern matching (MPM) [6].  
 468

469 Figure 2 shows a mosaic of chips (subimages  
 470 containing the detection) collected of a runner at about  
 471 135 meters. The chips are of size 29x24 which is very  
 472 small, on the order of 100 pixels on target. Performance on  
 473 only one observation per frame is mediocre, especially  
 474 when the runner is obscured by a brighter object as seen in  
 475 the first row of chips in the mosaic.  
 476

477 Figure 3 shows the result of multilook fusion using the  
 478 SPRT, Bayesian Fusion, and DS on the outputs of the  
 479 MPM GOF classifier. Since the MPM is designed to  
 480 produce  $N(0,1)$  scores for HOG features from a target,  
 481  $p(x_i|T)$  is set to  $N(0,1)$ . As discussed in Section 3 we use  
 482  $N(\mu_N, 1)$  for  $p(x_i|\bar{T})$  where  $\mu_N$  is empirically set to 5.  
 483 The desired error rates  $\alpha$  and  $\beta$  are set to  $1 \times 10^{-3}$ .  
 484

500  
501  
502  
503  
504  
505  
506  
507  
508  
509  
510  
511  
512  
513  
514515  
516 Figure 2: Infrared detections of a runner tracked in an uncooled  
517 infrared video imager.536  
537 Figure 3: Results of different multilook fusion algorithms of the  
538 runner GOF scores from runner chip sequence.539  
540 The black line in Figure 3 shows the SPRT cumulative  
541 log likelihood  $Z(n)$  (2) normalized by the upper SPRT  
542 threshold  $a$  (4). This puts the SPRT on the same scale as  
543 the Bayesian likelihood and DS BPA and gives a target /  
544 nontarget declaration when  $Z(n)/a$  passes  $1/-1$  (since  
545  $a=|b|$ ) . The green line shows the Bayesian likelihood  
546  $B(n)$  (7) with  $\lambda_0$  set to 1 (equal priors). The DS BPA is  
547 shown by three curves. The red curve is the BPA for the  
548  $T$  class  $m(T)$ , the blue curve is  $m(\bar{T})$ , and the magenta  
549 curve represents the uncertainty of the belief  $m(\Theta)$ .

Note that as the uncertainty  $m(\Theta)$  goes to zero the

550  
551 Bayesian likelihood  $B(n)$  approaches  $m(T)$ . Also when  
552 the current SPRT likelihood points to a nontarget or  
553  $Z(n)<0$  then  $m(T)<m(\bar{T})$  and then for  $Z(n)>0$   
554  $m(T)>m(\bar{T})$ . This supports the result in (28) that SPRT  
555 and DS make the same forced decision. There is also a  
556 similar relation between the Bayes likelihood  $B(n)$  and  
557  $Z(n)$ . When  $Z(n)<0$ ,  $B(n)<0.5$ , and  $Z(n)>0$ ,  
558  $B(n)>0.5$ . This becomes evident from (7) when  $\lambda_0=1$   
559 and the knowledge that  $Z(n)=0$  corresponds to  $\Lambda(n)=1$ .560  
561 It is interesting to note that between observation 30 and  
562 40 the DS uncertainty  $m(\Theta)$  is close to 0, but so is the  
563 SPRT log-likelihood. Any decision at this point would be  
564 an uninformed decision at low uncertainty. When  $Z(n)/a$   
565 goes above the threshold of 1, then we can make a high  
566 confidence decision that corresponds to low error rates of  
567  $\alpha$  and  $\beta$  set to  $1 \times 10^{-3}$ . Also note the Bayesian likelihood  
568 of  $B(n)$  and D.S. BPA  $m(T)$  of a target are very close to 1.569  
570 Figure 4 shows a mosaic of a chicken tracked by the  
571 system. The chip size is  $51 \times 34$ . Even though the chip size  
572 is different than that of the runner the use of the HOG  
573 features with the same number of horizontal and vertical  
574 blocks gives a system that is scale invariant.577  
578 Figure 4: Infrared detections of a chicken tracked in an uncooled  
579 infrared video imager.580  
581 Figure 5 shows the multilook fusion results for the  
582 tracked chicken against the upright-human dismounts  
583 classification system. When the SPRT log likelihood  
584  $Z(n)/a$  falls below the threshold of -1, we can make a  
585 nontarget decision with low error rates. Also  $B(n)$  and  
586  $m(\bar{T})$  go to zero indicating a nontarget.

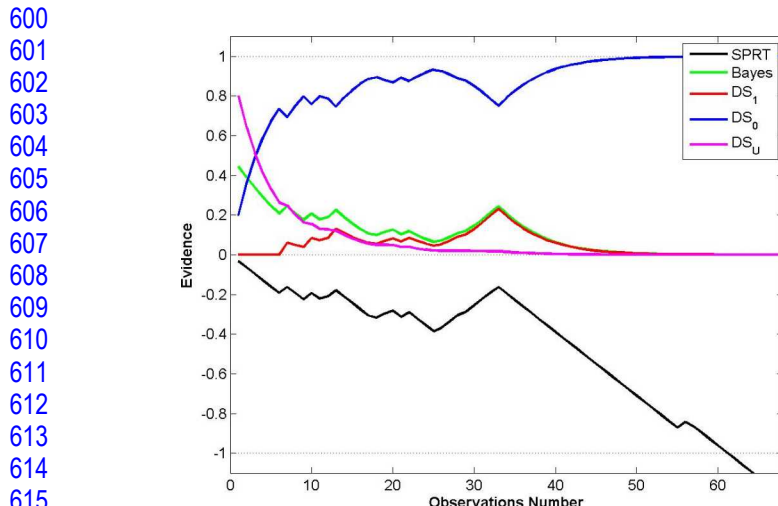


Figure 5: Results of different multilook fusion algorithms of the chicken GOF scores.

## 8. Conclusion

One of the main conclusions is that the sequential probability ratio test (SPRT), Bayesian fusion, and Dempster Shafer (DS) theory of evidence all make the same forced decision for the one-class problem when the consonant evidence is represented by probability density functions and there are equal priors for the target and nontarget classes. This is rather surprising, since Dempster Shafer incorporates the uncertainty of a belief in its belief combination rule.

While a one-class classifier approach may seem severely limiting one could solve the multi-class problem by designing a one-class classifier for each class.

Each fusion approach brings a different element to the problem of multiple look fusion. The SPRT approach allows one to select decision thresholds that control the two main errors used to measure a system's performance: the probability of missed detection and the probability of false alarm. Bayesian likelihoods become probabilities if the PDF's are discrete. Dempster Shafer incorporates belief uncertainty into evidence combination rule.

By theoretically analyzing each under a common probabilistic framework we are able to mathematically transform one into another and use or improve the best features of each.

## References

[1] E. Boult, X. Gao, R. Micheals, and M. Eckmann, "Omni-directional visual surveillance," *Image and Vision Computing*, vol. 22, pp. 515, 2004.

[2] N. Dalal, and B. Triggs, "Histogram of oriented gradients for human detection," *Computer Vision and Pattern Recognition Conference*, June 2005. 650  
651  
652  
653  
654  
655  
656  
657  
658  
659  
660  
661  
662  
663  
664  
665  
666  
667  
668  
669  
670  
671  
672  
673  
674  
675  
676  
677  
678  
679  
680  
681  
682  
683  
684  
685  
686  
687  
688  
689  
690  
691  
692  
693  
694  
695  
696  
697  
698  
699

[3] J. D. Gibson and J. L. Melsa, *Introduction to Nonparametric Detection with Applications*. New York: IEEE Press, pp. 25, 1996. 650  
651  
652  
653  
654  
655  
656  
657  
658  
659  
660  
661  
662  
663  
664  
665  
666  
667  
668  
669  
670  
671  
672  
673  
674  
675  
676  
677  
678  
679  
680  
681  
682  
683  
684  
685  
686  
687  
688  
689  
690  
691  
692  
693  
694  
695  
696  
697  
698  
699

[4] H. Kim, and P. H. Swain, "Evidential reasoning approach to multisource-data classification in remote sensing," *IEEE Transactions on Systems, Man, and Cybernetics*, **24**, No. 8, 1257-1265, 1995. 650  
651  
652  
653  
654  
655  
656  
657  
658  
659  
660  
661  
662  
663  
664  
665  
666  
667  
668  
669  
670  
671  
672  
673  
674  
675  
676  
677  
678  
679  
680  
681  
682  
683  
684  
685  
686  
687  
688  
689  
690  
691  
692  
693  
694  
695  
696  
697  
698  
699

[5] M. W. Koch, G. B. Haschke, and K. T. Malone, "Classifying acoustic signatures using the sequential probability ratio test," *Sequential Analysis Journal*, vol. 23, 4, pp. 557-583, 2004. 650  
651  
652  
653  
654  
655  
656  
657  
658  
659  
660  
661  
662  
663  
664  
665  
666  
667  
668  
669  
670  
671  
672  
673  
674  
675  
676  
677  
678  
679  
680  
681  
682  
683  
684  
685  
686  
687  
688  
689  
690  
691  
692  
693  
694  
695  
696  
697  
698  
699

[6] M. L. Koudelka, J. A. Richards, and M. W. Koch, "Multinomial pattern matching for high range resolution radar profiles," *Algorithms for Synthetic Aperture Radar Imagery XIV*. Edited by Zelnio, Edmund G.; Garber, Frederick D.. Proceedings of the SPIE, Volume 6568, pp. 65680V (2007). 650  
651  
652  
653  
654  
655  
656  
657  
658  
659  
660  
661  
662  
663  
664  
665  
666  
667  
668  
669  
670  
671  
672  
673  
674  
675  
676  
677  
678  
679  
680  
681  
682  
683  
684  
685  
686  
687  
688  
689  
690  
691  
692  
693  
694  
695  
696  
697  
698  
699

[7] M. Moya and D. Hush, "Network constraints and multi-objective optimization for one-class classification," *Neural Networks*, vol. 9, 3, pp. 463-474, 1996. 650  
651  
652  
653  
654  
655  
656  
657  
658  
659  
660  
661  
662  
663  
664  
665  
666  
667  
668  
669  
670  
671  
672  
673  
674  
675  
676  
677  
678  
679  
680  
681  
682  
683  
684  
685  
686  
687  
688  
689  
690  
691  
692  
693  
694  
695  
696  
697  
698  
699

[8] K. Murphy, and B. Myors, *Statistical Power Analysis: A Simple and General Model for Traditional and Modern Hypothesis Tests*. New Jersey: Lawrence Erlbaum Associates, 1998. 650  
651  
652  
653  
654  
655  
656  
657  
658  
659  
660  
661  
662  
663  
664  
665  
666  
667  
668  
669  
670  
671  
672  
673  
674  
675  
676  
677  
678  
679  
680  
681  
682  
683  
684  
685  
686  
687  
688  
689  
690  
691  
692  
693  
694  
695  
696  
697  
698  
699

[9] J. Savage, et. al., "Irma 5.2 multi-sensor signature prediction model," Proc. SPIE 6564, Modeling and Simulation for Military Operations II, April 2007. 650  
651  
652  
653  
654  
655  
656  
657  
658  
659  
660  
661  
662  
663  
664  
665  
666  
667  
668  
669  
670  
671  
672  
673  
674  
675  
676  
677  
678  
679  
680  
681  
682  
683  
684  
685  
686  
687  
688  
689  
690  
691  
692  
693  
694  
695  
696  
697  
698  
699

[10] Shafer, G., *A Mathematical Theory of Evidence*, Princeton University Press, 1976. 650  
651  
652  
653  
654  
655  
656  
657  
658  
659  
660  
661  
662  
663  
664  
665  
666  
667  
668  
669  
670  
671  
672  
673  
674  
675  
676  
677  
678  
679  
680  
681  
682  
683  
684  
685  
686  
687  
688  
689  
690  
691  
692  
693  
694  
695  
696  
697  
698  
699

[11] A. Wald, *Sequential Analysis*, John Wiley & Sons Inc, New York, 1947. 650  
651  
652  
653  
654  
655  
656  
657  
658  
659  
660  
661  
662  
663  
664  
665  
666  
667  
668  
669  
670  
671  
672  
673  
674  
675  
676  
677  
678  
679  
680  
681  
682  
683  
684  
685  
686  
687  
688  
689  
690  
691  
692  
693  
694  
695  
696  
697  
698  
699